# Kinetic energy distributions of the fragment ions from multiply ionized CH as functions of the charge state of the intermediate states



Yoshida, S.; Majima, T.; Tsuchida, H.; Saito, M.

# Kinetic energy distributions of the fragment ions from multiply ionized $C_2H_6$ as functions of the charge state of the intermediate states

S. Yoshida[a], T. Majima[a*], H. Tsuchida[b], and M. Saito[a]

[a] *Department of Nuclear Engineering, Kyoto University, Kyoto 606-8501, Japan*

[b] *Quantum Science and Engineering Center, Kyoto University, Uji 611-0011, Japan*

*Corresponding author: majima@nucleng.kyoto-u.ac.jp

## Abstract

Here, we report the kinetic energy distributions (KEDs) of the fragment ions produced from multiply ionized ethane ($C_2H_6$) molecules in single electron capture collisions with 1.2 MeV $C^{2+}$. To systematically investigate the fragmentation dynamics, the KEDs were obtained as functions of the charge state of the intermediate $C_2H_6^{r+*}$ ions $r$ transiently generated prior to fragmentation. $r$ was determined from coincidence measurement of the fragment ions and the number of emitted electrons. The KEDs are drastically different depending on the number of broken C–H bonds. The underlying causes are explained by the variation of the relative contributions of the multiply ionized states and preferential fragmentation pathways. For instance, $CH_n^+$ fragment ions with smaller $n$ exhibit lower KEs because they are likely to be correlated with $H^+$ emission, which

carries away a large portion of the KE release. In addition, we report the KEDs of $H_3^+$ produced from doubly and triply charged states.

*Keywords: molecular fragmentation; multiple ionization; fast ion collisions, kinetic energy distributions, ethane*

## 1. Introduction

Multiple ionization of molecules is induced by strong electric fields generated by intense short laser pulses, collisions of highly charged ions, and swift heavy ions.[1–3] Highly ionized molecules dissociate or "Coulomb explode" into fragments with high kinetic energies (KEs). Understanding the fragmentation mechanisms is of fundamental interest in molecular sciences and related fields, such as radiation physics and chemistry. Although the fragmentation processes of various molecules have been extensively studied, most studies have focused on specific pathways, such as two- or three-body fragmentation, which can be analyzed from coincidence detection of the fragment ions. Analysis of the product ions from larger molecules becomes difficult because larger numbers of ions can be produced from a single molecule. Possible production of neutral fragments further complicates the situation. The overall picture of the fragmentation processes of multiply charged polyatomic molecules is thus still unclear. The electron counting technique developed by Martin et al.[4] can be used to systematically investigate fragmentation of multiply ionized molecules in fast heavy ion collisions. Coincidence measurements of the number of emitted electrons provide information about the product ion species as functions of the degree of multiple ionization irrespective of the number of fragments, including neutral fragments. We have previously revealed the fragmentation patterns from the multiply ionized states of various polyatomic molecules.[5–8]

Recently, we implemented a momentum imaging technique to systematically investigate the KE distributions (KEDs) of product ions as functions of the intermediate charge state. In a previous study, we demonstrated a measurement with an acetylene ($C_2H_2$) target.[9] In this work, we extend the study to ethane ($C_2H_6$), which contains

more hydrogen atoms than acetylene. Examination of the KEDs with respect to the number of broken C–H bonds reveals the role of hydrogen emission in the fragmentation dynamics. In addition, $H_3^+$ emission was investigated as a characteristic product ion from multiply charged $C_2H_6$.

## 2. Experimental method

The experiment was performed at the 1.7 MV tandem accelerator facility of the Quantum Science and Engineering Center, Kyoto University. The experimental procedure was essentially the same as in our previous study.[9] Thus, only the relevant aspects will be outlined here. A well-collimated beam of 1.2 MeV $C^{2+}$ was incident on the $C_2H_6$ gas target. To select the single electron capture collisions, the outgoing $C^+$ ions were separated from the other charge states ($C^{q+}$, $q \neq 1$) by an electrostatic deflector and selectively detected by a semiconductor detector ($SSD_p$). The signals from the $SSD_p$ were used as the trigger of the following measurements. The electrons emitted in the collisions were detected by another semiconductor detector ($SSD_e$). The $SSD_e$ was placed on a +25 kV high voltage stage to accelerate the electrons to the detectable energy of 25 keV. Pulse height analysis of the $SSD_e$ signals provides information about the number of electrons emitted in each collision event $n_e$ because the pulse height corresponds to $25n_e$ keV. In the single electron capture condition, the charge state of the intermediate $C_2H_6^{r+*}$ ion can be determined by $r = n_e + 1$. The product ions were extracted to a linear time-of-flight (TOF) mass spectrometer based on the velocity map imaging technique[10] and detected by a multichannel plate (MCP) detector combined with a position-sensitive delay-line anode. Examples of the two-dimensional images of $C_2H_6^+$, $C_2^+$, $CH_3^+$, and $H^+$ on the MCP detector are shown in Fig. 1. The distance from

the center position represents the KE of the product ion in the direction parallel to the detector plane. Intact $C_2H_6^+$ ions form a small spot because of negligibly small momentum transfer. The full width at half maximum of the $C_2H_6^+$ spot is less than 1.4 mm. The lighter fragment ions spread to larger regions because of their higher KEs received during fragmentation. The image of $CH_3^+$ has a structure with an outer ring and a central spot. This indicates that the KE distribution of $CH_3^+$ consists of two main components, which will be discussed in Section 3.2. The three-dimensional momentum of each product ion was obtained from the TOF and the position on the MCP detector. The ion signals were recorded together with the pulse height of the $SSD_e$ signal event by event, which allows the fragmentation pattern[5–8] and momentum of each product ion[9] to be analyzed as a function of the charge state of the intermediate $C_2H_6^{r+*}$ ion.

## 3. Results and discussion

### 3.1. KEDs of $C_2H_n^+$ ($n$ = 0–6)

The KEDs of the product ions of $C_2H_n^+$ for $n$ = 0–6 produced by emission of neutral and ionized hydrogen species are plotted as “total” distributions in Fig. 2. The widths of the total distributions are substantially different for $n \geq 4$ and $n \leq 3$. The $C_2H_n^+$ ions for $n \geq 4$ have low KEs below 0.3 eV, while those for $n \leq 3$ spread up to about 1 eV. To understand the underlying causes, the contributions from the different charge states of the intermediate $C_2H_6^{r+*}$ ions are also plotted in the figures. They clearly show that the large broadening of the total KEDs for $n \leq 3$ is caused by the contributions of the multiply ionized states ($r \geq 2$).

$C_2H_5^+$ and $C_2H_4^+$ do not gain large KEs because they are almost exclusively produced from the singly charged intermediate ions ($r$ = 1) through emission of neutral

hydrogen species. As mentioned in a previous paper,[7] $C_2H_5^+$ and $C_2H_4^+$ are expected to be produced from singly charged $C_2H_6^{+*}$ excited states with low energy barriers according to the appearance energies of 11.46, 12.7, and 11.90 eV for production of $C_2H_6^+$, $C_2H_5^+ + H$, and $C_2H_4^+ + H_2$, respectively.[11] Comparing the KEDs of $C_2H_n^+$ for $r = 1$, the KED becomes broader with decreasing $n$. This shows that higher internal excitation is involved in emission of more neutral hydrogen.

$C_2H_n^+$ with $n \leq 3$ can gain larger KEs because of the contributions of the multiply charged intermediate states ($r \geq 2$) as significant production channels. Coulomb repulsion from the other fragment ions enhances the KEs of $C_2H_n^+$. Moreover, the contributions from higher charge states ($r \geq 3$) increase with decreasing $n$. However, in this regard, the KEs for $r \geq 3$ do not further broaden even as $r$ increases in contrast to the expectation from a higher Coulomb potential. Increase of fragment hydrogen ions does not enhance the KEs of $C_2H_n^+$, probably because the Coulomb repulsive forces are somewhat canceled by the symmetric geometrical distribution of the hydrogen atoms. In a previous paper, a simpler example of reduction of the KE owing to symmetric fragmentation was reported for acetylene with the following pathway: $C_2H_2^{3+} \rightarrow H^+ + C_2^+ + H^+$.[9]

### 3.2. KEDs of $CH_n^+$ ($n$ = 0–3)

The KEDs of $CH_n^+$ for $n$ = 0–3, which are produced through C–C bond breaking, are shown in Fig. 3. The total distributions extend up to about 6 eV. The shapes of the distributions are greatly different for different $n$. This can be attributed to variation of the distributions for specific $r$ and their relative fractions depending on $n$. Note that the sharp peak at around 0 eV in the KED of $CH_2^+$ comes from $r = 2$. This component can

be ascribed to metastable $C_2H_4^{2+}$, rather than $CH_2^+$, because the distribution is nearly equivalent to those of $C_2H_n^+$ for $n \geq 4$. In contrast, the KED of $CH_3^+$ for $r = 2$ has no strong peak at around 0 eV. This means that doubly charged intact $C_2H_6^{2+*}$ ions cannot survive during the TOF measurements. They dissociate because of the low energy barrier for $H_2$ emission and are stabilized by $H_2$ emission.

Unlike the KED of $CH_2^+$, the low-energy peak at around 0 eV in the KED of $CH_3^+$ originates from $r = 1$. It has a peak at less than 0.5 eV. The KEDs of $CH_2^+$, $CH^+$, and $C^+$ for $r = 1$ have no sharp peak in this energy range and exhibit broad distributions up to about 3 eV. This indicates that the fragmentation pathway

$$C_2H_6^{+*} \rightarrow CH_3^+ + [C, 3H] \quad (1)$$

has a lower KE release (KER) originating from lower excited states compared with the pathways

$$C_2H_6^{+*} \rightarrow CH_n^+ (n \leq 2) + [C, (6 - n)H]. \quad (2)$$

Note that [C, 3H] and [C, (6 – *n*)H] just indicate the constituent atoms of the neutral fragments because their molecular compositions are unknown. These results are consistent with the KEDs reported in an electron impact experiment.[12] At electron energies below the threshold of double ionization, the KE of $CH_3^+$ is distributed below 0.5 eV and the $CH_2^+$ ions have KEs ranging up to more than 1 eV. They agree well with the present results for $r = 1$. In addition, another component at around 2 eV starts to appear at electron energies higher than 30 eV. The present results elucidate that these high-energy components are contributions from doubly charged intermediate ions ($r = 2$).

Except for the sharp peaks at around 0 eV, the large differences in the total KEDs are mainly because of the differences in the distributions for $r = 2$ and 3. In the KEDs of

$CH^+$ and $C^+$, the peak at around 2.5 eV decreases with decreasing $n$ and a lower energy peak appears at around 0.5 eV. To investigate the origin of the differences in the KEDs, the distributions at $r$ = 2 are separately plotted in Fig. 3(e)–(h) for the following fragmentation pathways:

$$C_2H_6^{2+*} \rightarrow CH_n^+ + CH_m^+ \ (m = 0–3) + [(6 – n – m)H], \quad (3)$$

$$C_2H_6^{2+*} \rightarrow CH_n^+ + H^+ + [C, (5 – n)H]. \quad (4)$$

Fragmentation pathways (3) and (4) provide the peaks at the higher (~2.5 eV) and lower (~0.5 eV) energies, respectively. It is unsurprising that the KEs of $CH_n^+$ differ depending on the other simultaneously produced ion ($CH_m^+$ or $H^+$). They are qualitatively reasonable considering momentum conservation of the two fragment ions. The important point is that the predominant pathway shifts from (3) to (4) as $n$ decreases. We found that $CH_3^+$ is rarely correlated with $H^+$. With decreasing $n$, the probability of $H^+$ production is enhanced. As a result, $CH_n^+$ becomes preferentially correlated with $H^+$. This example clearly demonstrates that multifragmentation caused by a high internal energy does not always lead to an increase in the KEs, as in the case of emission of $C^+$ fragment ions. It strongly depends on the fragmentation mechanism. In the present example, enhancement of C–H bond breaking leads to reduction of the KEs of $CH_n^+$ because $H^+$ removes a large fraction of the KER.

The same explanation applies to the KEDs for $r$ = 3 with the following pathways:

$$C_2H_6^{3+*} \rightarrow CH_n^+ + CH_m^+ + H^+ + [(5 – n – m)H], \quad (5)$$

$$C_2H_6^{3+*} \rightarrow CH_n^+ + 2H^+ + [C, (4 – n)H]. \quad (6)$$

The KEDs of $CH_n^+$ for $r$ = 3 do not show a large increase in the KEs compared with $r$ = 2. This means that additional $H^+$ emission does not greatly enhance the KEs of $CH_n^+$. One reason is that $CH_n^+$ receive a small recoil from $H^+$ emission owing to the large

difference in mass between $CH_n^+$ and $H^+$. In other words, most of the additional potential energy is removed by the fast $H^+$ emission. The other reason is the geometrical effect. The additional $H^+$ emission does not always act in the direction of the increase in the KE of $CH_n^+$, as is the case with $C_2H_n^+$ discussed in Section 3.1. Following the above discussion, we expect that the KE of $CH_n^+$ does not greatly increase even for $r > 3$ unless a multiply charged $C^{q+}$ fragment ion ($q \geq 2$) is produced.

### 3.3. KEDs of $H_n^+$ ($n$ = 1–3)

The KEDs of $H_n^+$ for $n$ = 1–3 are shown in Fig. 4. All of the total KEDs have a peak at around 4 eV. The peak positions are consistent with the results reported by infrared femtosecond laser irradiation, where the KEs of $H^+$, $H_2^+$, and $H_3^+$ produced in two-body fragmentation of $C_2H_6$ are 3.5, 3.5, and 3.6 eV, respectively.[13] The peak width of the $H^+$ distribution is much broader than those of $H_3^+$ and $H_2^+$. As previously reported,[7] $H_3^+$ is predominantly produced from the doubly charged $C_2H_6^{2+*}$ ion. The distribution is narrower than the KED of $H^+$ for $r$ = 2, indicating that $H_3^+$ is produced through excited states in a specific energy range. A small fraction of the $H_3^+$ ions are produced from $r$ = 3. The small change of the mean KEs from $r$ = 2 indicates a sequential fragmentation mechanism following prompt $H^+$ emission. Similar behavior is observed in the KEDs of $H_2^+$.

In contrast to $H_3^+$ and $H_2^+$, $H^+$ ions are generated from a wide range of charge states. To compare the structures of the KEDs at different $r$, the distributions normalized by each maximum intensity are plotted in Fig. 4(d). The peak positions greatly shift from $r$ = 1 to 2, and the distribution becomes broader and extends to a higher KE with increasing $r$. It is reasonable for the KEDs of $H^+$ to directly reflect an increase in the

Coulomb potential because other fragments do not interfere with prompt $H^+$ ejection.

## 4. Summary

We have performed KED measurements of the fragment ions generated from multiply ionized $C_2H_6$ ions in single electron capture collisions with 1.2 MeV $C^{2+}$. The KEDs were systematically obtained as functions of the charge state of the intermediate ions $C_2H_6^{r+*}$ ions $r$ by performing a coincidence measurement of the number of emitted electrons. The KEDs show that the substantial differences of the total KEDs of $C_2H_n^+$ for $n$ = 3 and 4 are because of the contributions of the multiply charged intermediate states ($r \geq 2$). We found that the differences in the KEDs of $CH_n^+$ for different $n$ can be attributed to the different preferential fragmentation pathways. In particular, an increase in $H^+$ emission leads to reduction of the KEs of $CH_n^+$. In addition, the narrower KEDs of $H_3^+$ and $H_2^+$ compared with that of $H^+$ are probably because they are produced through specific excited states. In contrast to the other fragment ions, the KEs of $H^+$ are found to increase as functions of $r$ in a straightforward manner.

## Acknowledgments

This work was supported by JSPS KAKENHI (Grants Nos. 23760826 and 16K05015). We also thank M. Naito and Y. Sasaki for their technical support during the experiment.

# List of references

[1] D. Mathur, *Phys. Rep.* **2004**, *391*, 1.

[2] L. Adoui et al., *Nucl. Instr. Meth. Phys. Res. B* **2006**, *245*, 94.

[3] T. Yatsuhashi, N. Nakashima, J. Photochem. Photobiol. C **2018**, *34*, 52.

[4] S. Martin, L. Chen, A. Denis, J. Désesquelles, *Phys. Rev. A* **1998** *57*, 4518.

[5] T. Majima Y. Nakai H. Tsuchida, A. Itoh, *Phys. Rev. A* **2004**, *69*, 031202(R).

[6] T. Majima, Y. Nakai, T. Mizuno, H. Tsuchida, A. Itoh, *Phys. Rev. A* **2006**, *74*, 033201.

[7] T. Majima, T. Murai, T. Kishimoto, Y. Adachi, S. O. Yoshida, H. Tsuchida, A. Itoh, *Phys. Rev. A* **2014**, *90*, 062711.

[8] T. Majima, T. Murai, S. Yoshida, M. Saito, H. Tsuchida, A. Itoh, *Int. J. Mass Spectrom.* **2017**, *421*, 25.

[9] S. Yoshida, T. Majima, T. Asai, M. Matsubara, H. Tsuchida, M. Saito, A. Itoh, *Nucl. Instr. Meth. Phys. Res. B* **2017**, *408*, 203.

[10] D. H. Parker, A. T. J. B. Eppink, *J. Chem. Phys.* **1997**, *107*, 7.

[11] E. Vašeková, M. Stano, Š. Matejčík, J. D. Skalný, P. Mach, J. Urban, and T. D. Märk, *Int. J. Mass Spectrom*. **2004**, *235*, 155.

[12] C. Tian, C. R. Vidal, *J. Chem. Phys.* **1998**, *109*, 1704.

[13] K. Hoshina, H. Kawamura, M. Tsuge, M. Tamiya, M. Ishiguro *J. Chem. Phys.* **2011**, *134*, 064324.

# List of figure captions

Figure 1. Two-dimensional images of the (a) $C_2H_6^+$, (b) $C_2^+$, (c) $CH_3^+$, and (d) $H^+$ product ions on the MCP detector. The projections onto the *x* and *y* axes are plotted for $C_2H_6^+$.

Figure 2. (a)–(g) KEDs of $C_2H_n^+$ ($n$ = 0–6) and the contributions of the specific charge states of the intermediate $C_2H_6^{r+*}$ ion ($r$ = 1–4).

Figure 3. (a)–(d) KEDs of $CH_n^+$ ($n$ = 0–3) and the contributions of the specific charge states of the intermediate $C_2H_6^{r+*}$ ion ($r$ = 1–4). Note that (b) includes $C_2H_4^{2+}$. (e)–(h): KEDs for $r$ = 2 separated by the two fragmentation pathways $CH_n^+ + CH_m^+$ and $CH_n^+ + H^+$.

Figure 4. (a)–(c) KEDs of $H_n^+$ ($n$ = 0–3) and the contributions of the specific charge states of the intermediate $C_2H_6^{r+*}$ ion ($r$ = 1–4). (d) Distributions of $H^+$ for $r$ = 1–4 normalized by each maximum intensity.

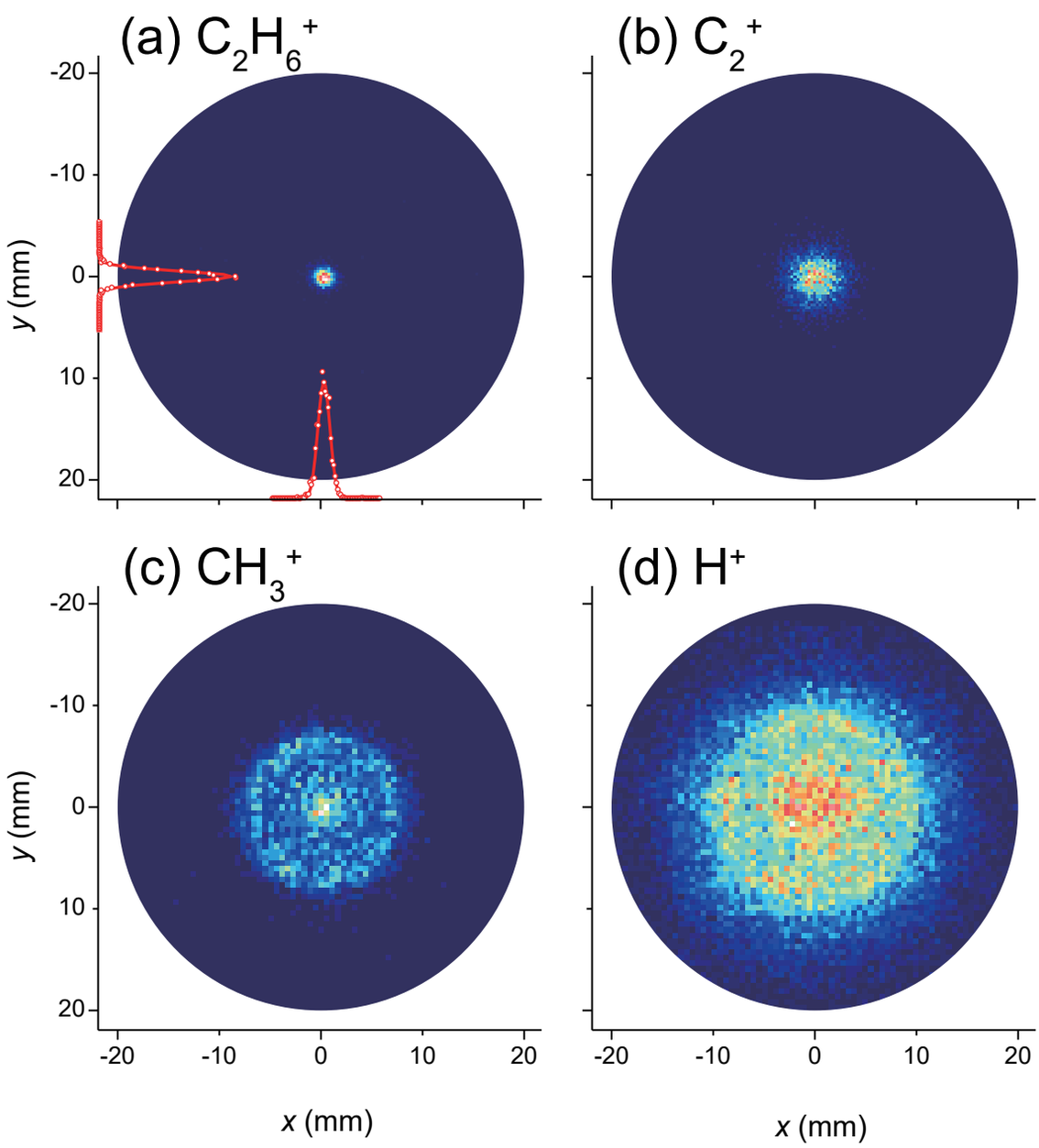


Fig.1

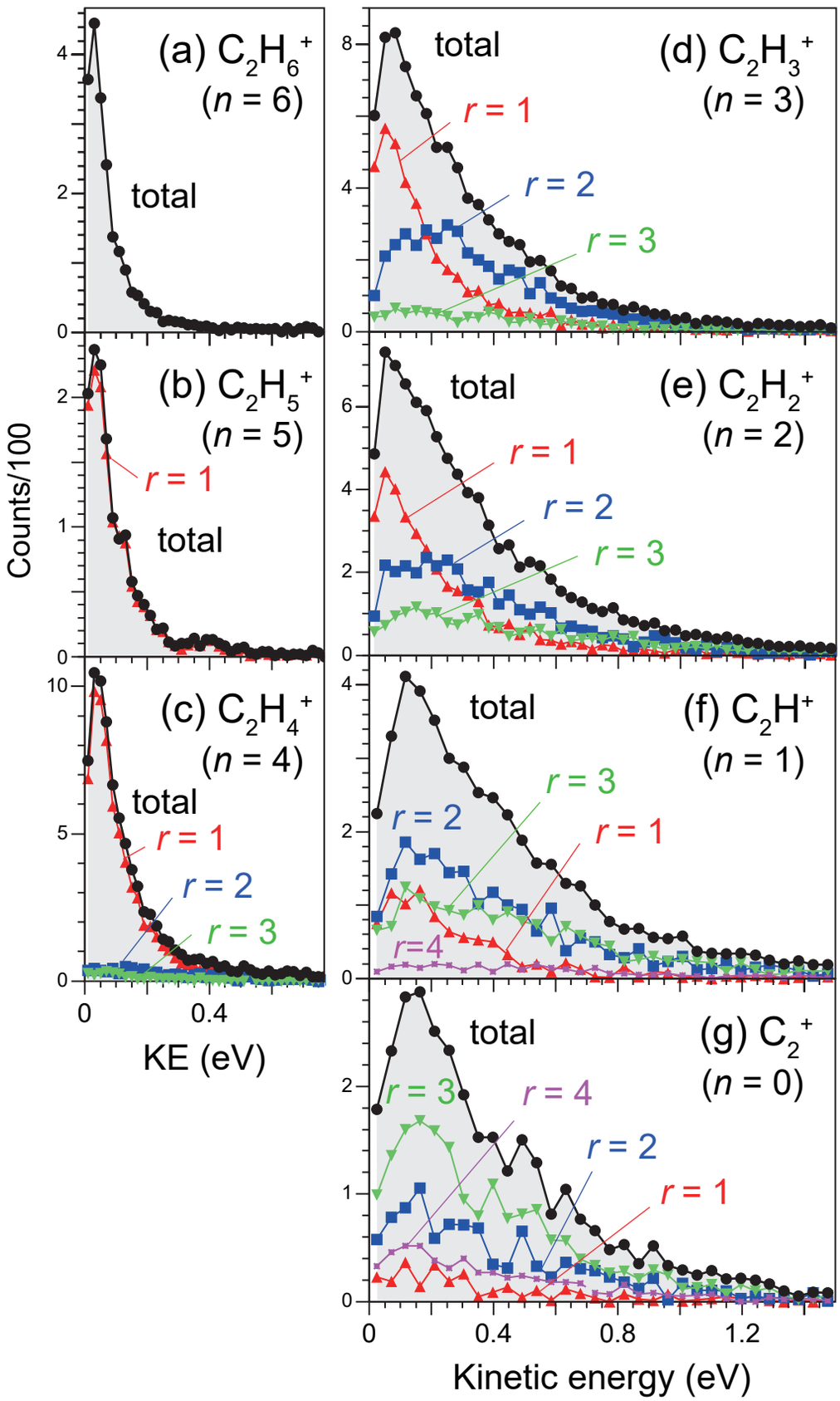


Fig.2

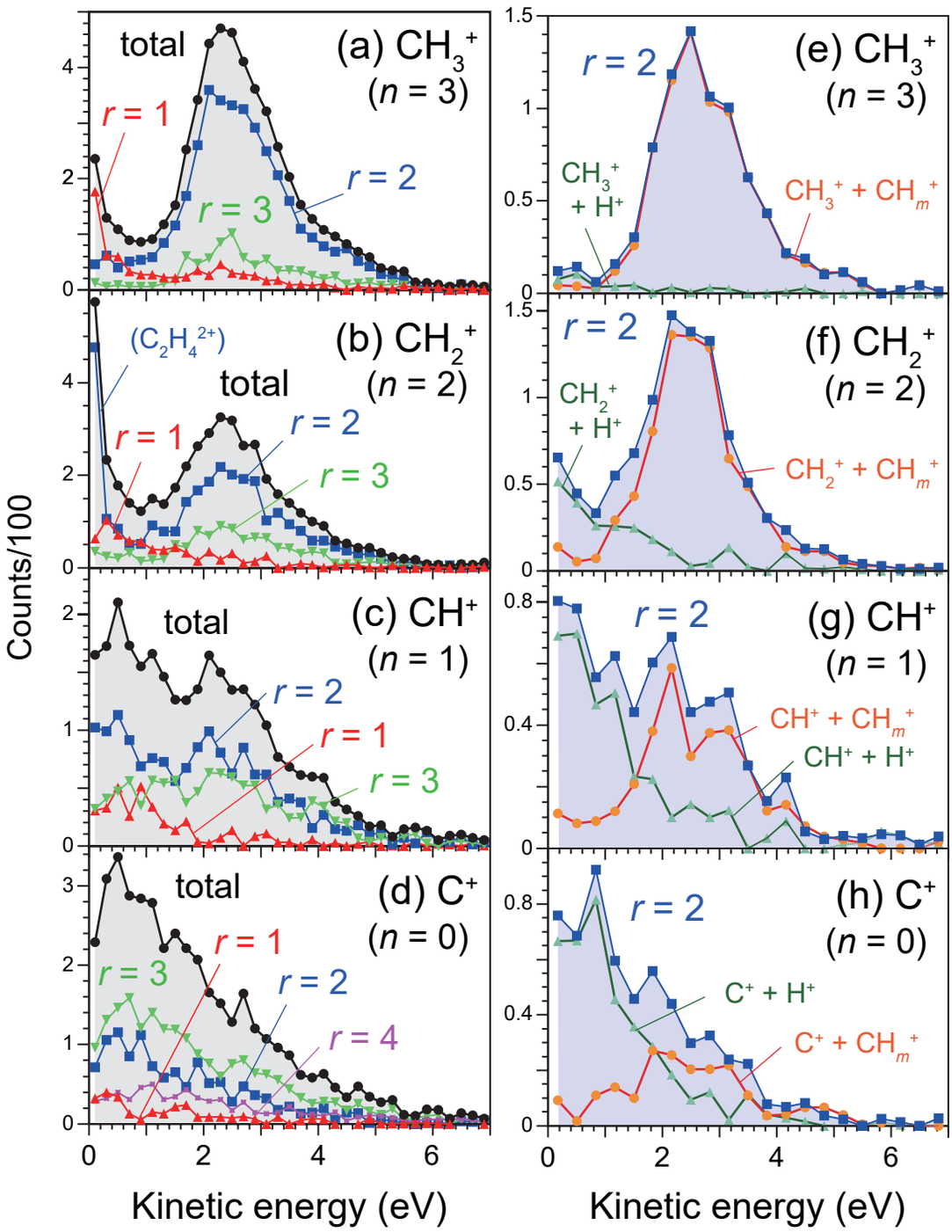


Fig.3

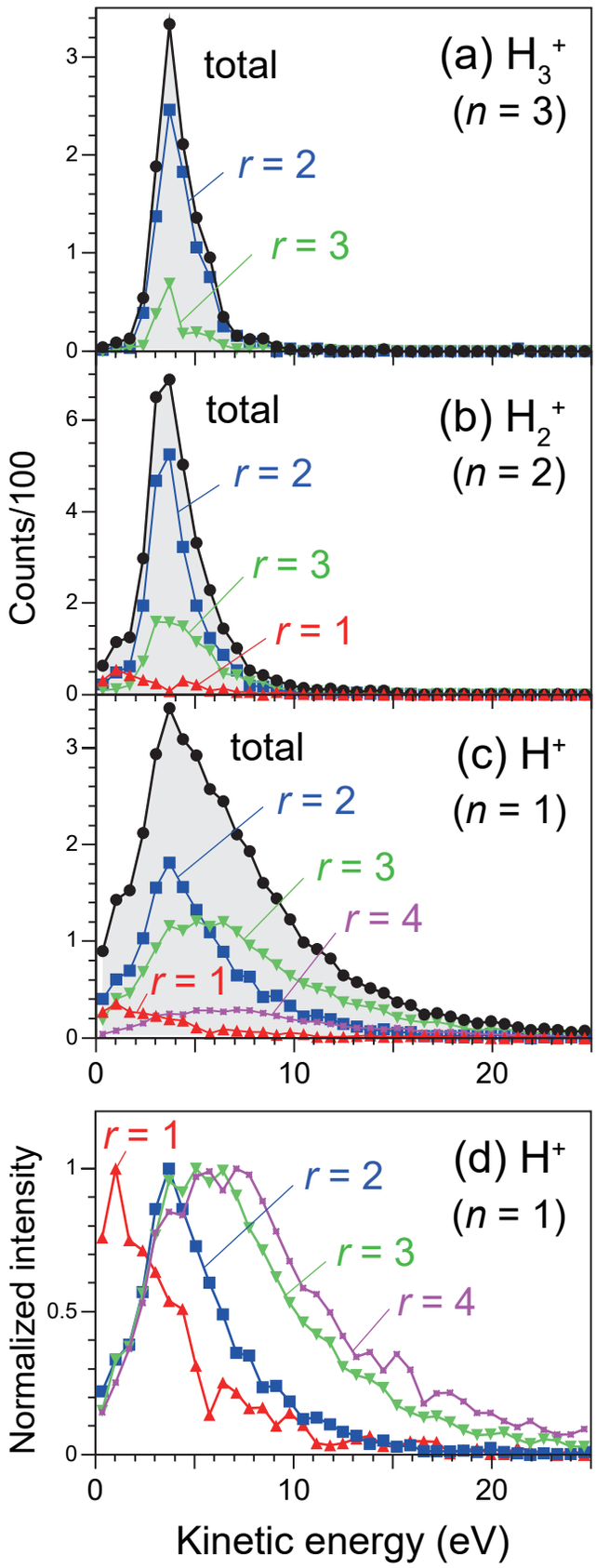


Fig.4